

Synthesis, Structures, and Electrochemistry of Gold(III) Ethylenediamine Complexes and Interactions with Guanosine 5'-Monophosphate

Shourong Zhu,[†] Waldemar Gorski,[†] Douglas R. Powell,[‡] and Judith A. Walmsley^{*†}

Department of Chemistry, The University of Texas at San Antonio, 6900 North Loop 1604 West, San Antonio, Texas 78249-0698, and Department of Chemistry, University of Kansas, Lawrence, Kansas 66045-7582

Received August 18, 2005

[Au(en)Cl₂]Cl·2H₂O, where en = ethylenediamine (1,2-diaminoethane), has been synthesized, and its structure has been solved for the first time by the single-crystal X-ray diffraction method. The complex has square-planar geometry about Au^{III}, and the anionic Cl⁻ is located in the apical position and at a distance of 3.3033(10) Å compared to 2.2811(9) and 2.2836(11) Å for the coordinated Cl⁻. [Au(en)Cl₂]Cl·2H₂O belongs to the space group *Pbca* with *a* = 11.5610(15) Å, *b* = 12.6399(17) Å, *c* = 13.2156(17) Å, $\alpha = \beta = \gamma = 90^\circ$, and *Z* = 8. Bond lengths of Au–N are 2.03 Å. [Au(en)Cl₂]Cl·2H₂O is less thermally stable than [Au(en)₂]Cl₃ because of the replacement of two Cl ligands by a second en ligand in the latter. Cyclic voltammetry shows that the formal potential of Au^{III}/Au⁰ becomes more negative in the series [AuCl₄]⁻, [Au(en)Cl₂]⁺, and [Au(en)₂]³⁺. ¹H, ¹³C, and ³¹P NMR reveal that in an aqueous solution [Au(en)Cl₂]⁺ bonds to guanosine 5'-monophosphate, 5'-GMP (1:1 mole ratio), via N(7), although the stability is not very high. NMR data also indicate that N(7)–O(6) or N(7)–phosphate 5'-GMP chelation, as found in some gold(III) nucleotide complexes, is not present. The gold(III) complex undergoes hydrolysis at pH >2.5–3.0 and, therefore, N1 coordination to 5'-GMP is not observed. No direct coordination between 5'-GMP and [Au(en)₂]Cl₃ is observed.

Introduction

Gold(III) complexes are isoelectronic and generally isostructural to platinum(II) complexes, and therefore it is anticipated that they will have activity similar to that of platinum(II) antitumor drugs.^{1–5} However, compared to the corresponding platinum(II) complexes, gold(III) complexes have not been well explored chemically or electrochemically possibly because few gold(III) complexes have been shown to be sufficiently stable in aqueous solution.^{6,7}

Ethylenediamine (en) is a common chelating ligand that is widely used in transition-metal complexes. Its gold complexes have been known since 1931,^{8–10} and the crystal structure of [Au(en)₂Cl₂]Cl was determined.¹¹ This complex has a square-bipyramidal geometry with two Cl at the apical positions. [Au(en)Cl₂]Cl was reported to be isolated in 1967 by Brodersen and Kahlert.¹² However, the crystal structure for this 1:1 complex, as well as the electrochemical properties and reactivity with guanosine 5'-monophosphate (5'-GMP; Figure 1) for both [Au(en)Cl₂]Cl and [Au(en)₂Cl₂]Cl, is first reported herein.

* To whom correspondence should be addressed. E-mail: judith.walmsley@utsa.edu.

[†] The University of Texas at San Antonio.

[‡] University of Kansas.

- Messori, L.; Marcon, G. *Met. Ions Biol. Syst.* **2004**, *42*, 385–424.
- Messori, L.; Marcon, G.; Orioli, P. *Bioinorg. Chem. Appl.* **2003**, *1*, 177–187.
- Tiekink, E. R. T. *Gold Bull. (London)* **2003**, *36*, 117–124.
- Zhang, C. X.; Lippard, S. J. *Curr. Opin. Chem. Biol.* **2003**, *7*, 481–489.
- Marcon, G.; Carotti, S.; Coronello, M.; Messori, L.; Mini, E.; Orioli, P.; Mazzei, T.; Cinellu, M. A.; Minghetti, G. *J. Med. Chem.* **2002**, *45*, 1672–1677.
- Abbate, F.; Orioli, P.; Bruni, B.; Marcon, G.; Messori, L. *Inorg. Chim. Acta* **2000**, *311*, 1–5.

- Fry, F. H.; Hamilton, G. A.; Turkevich, J. *Inorg. Chem.* **1966**, *5*, 1943–1946.
- Gibson, C. S.; Colles, W. M. *J. Chem. Soc.* **1931**, 2407–2416.
- Block, B. P.; Bailar, J. C., Jr. *J. Am. Chem. Soc.* **1951**, *73*, 4722–4725.
- Makotchenko, E. V. *Russ. J. Coord. Chem.* (translation of *Koord. Khim.*) **2003**, *29*, 720–723.
- Minacheva, L. K.; Gladkaya, A. S.; Sakharova, V. G.; Don, G. M.; Shchelokov, R. N.; Porai-Koshits, M. A. *Zh. Neorg. Khim.* **1988**, *33*, 683–687.
- Brodersen, K.; Kahlert, T. *Z. Anorg. Allg. Chem.* **1967**, *355*, 323–327.

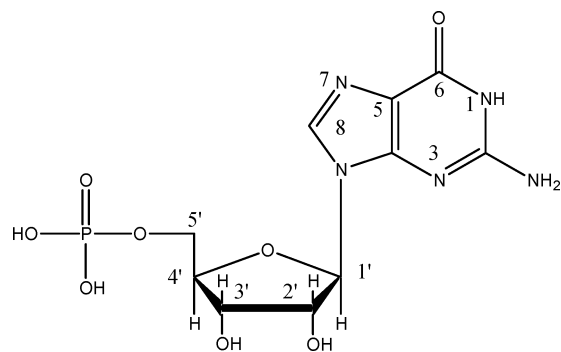


Figure 1. Guanylic acid, $H_2(5'-GMP)$.

Interest in the reactions of nucleobases, nucleosides, and nucleotides on gold surfaces has received considerable attention. Relatively few studies have been directed toward the isolation and characterization of these compounds with gold(III). Reaction of $AuCl_4^-$ with a variety of nucleosides and nucleotides has shown that the bonding mode of gold(III) is dependent upon the nucleoside or nucleotide. On the basis of solution studies, possible N(7)–O(6) chelation is suggested for guanosine and possible N(7)–phosphate macrochelation for 5'-GMP.^{13,14} Mixed-ligand complexes have been reported, such as $[Au(L-N,N')(5'-GMP)_2]$, where L is *N*-(4-methylphenyl-2-pyridinecarboxamide),¹⁵ and the dimethylgold complex, $[(CH_3)_2AuCl(\text{guanosine})]$.¹⁶

Cytotoxicity studies of gold(III) complexes of polydentate amines, including en, have shown that they are as effective against certain tumor cell lines as, or even more effective than, *cis*-platin.¹ When tested against *cis*-platin-resistant cell lines, the gold(III) complexes remained nearly as effective as against nonresistant cell lines. It was also shown that the bis(ethylenediamine)gold(III) complex binds to calf thymus DNA noncovalently, most probably through electrostatic interactions.¹⁷

Our interest has been the cyclic polynuclear complexes of the d^8 metal ions, especially those in which the metal ions are bridged by nucleotides. Complexes of $[Pd(en)]^{2+}$ with purine nucleotides, in which the nucleotide uses two N donor sites [N(7) and N(1)] to bridge between the palladium(II) centers, have been shown to be cyclic tetramers in aqueous solution.^{18,19} However, we have not found any evidence for cyclic species in the $[Au(en)Cl_2]^+$ system so far. Herein we report the synthesis of $[Au(en)Cl_2]Cl \cdot 2H_2O$ and $[Au(en)_2]Cl_3$, their thermogravimetric and electrochemical properties, reactions with 5'-GMP in solution, and the crystal structure of $[Au(en)Cl_2]Cl \cdot 2H_2O$.

Methods and Materials

Materials. $NaAuCl_4 \cdot 2H_2O$, ethylenediamine (en), D_2O , and $DMSO-d_6$ were purchased from Aldrich Chemical Co. and used as received. $H_2(5'-GMP)$ and $Na_2(5'-GMP)$ were purchased from Sigma and used as received. All solutions other than those for NMR measurements were prepared using deionized water that was purified with a Barnstead NANOpure cartridge system (18 M Ω).

Syntheses. (i) $[Au(en)Cl_2]Cl \cdot 2H_2O$. $NaAuCl_4 \cdot 2H_2O$ (0.218 g, 0.548 mmol) was dissolved in 20 mL of absolute ethanol at room temperature. To this solution was added 37 μ L of en (0.55 mmol). An orange-brown precipitate formed immediately. After the mixture was stirred for 20 min, the precipitate disappeared and the solution became slightly turbid. After filtration, the solution was concentrated to 5 mL and left to stand at room temperature. Pale yellow crystals of $[Au(en)Cl_2]Cl \cdot 2H_2O$ formed gradually. Yield: 0.15 g (68%). Elem anal. Calcd for $[Au(en)Cl_2]Cl \cdot 2H_2O$: C, 6.01; H, 3.03; N, 7.01; Cl, 26.63. Found: C, 6.11; H, 2.97; N, 6.94, Cl, 26.71. 1H NMR: 3.30 ppm in D_2O . The complex darkens in color at 105 °C and decomposes at 195 °C.

(ii) $[Au(en)_2]Cl_3 \cdot 0.5HCl$. $NaAuCl_4 \cdot 2H_2O$ (0.20 g, 0.50 mmol) was dissolved in 5 mL of deionized H_2O . To this solution was added 1.0 mL of a 1.0 M aqueous solution of en. An orange precipitate formed at once and gradually redissolved (pH 4.3). A trace amount of undissolved precipitate was removed by filtration, and 30 mL of ethanol was added to the filtrate. The very pale yellow precipitate, which formed immediately, was filtered off and air-dried. Yield: 0.16 g (72%). Elem anal. Calcd for $[Au(en)_2]Cl_3 \cdot 0.5HCl$: C, 10.87; H, 3.76; N, 12.69; Cl, 28.09. Found: C, 11.45; H, 3.72; N, 12.98, Cl, 27.87. 1H NMR: 3.27 ppm in D_2O . The complex darkens in color at 170 °C and decomposes at 195 °C.

(iii) Nucleotide Stock Solutions. $Na_2(5'-GMP)$ or $H_2(5'-GMP)$ was dissolved in H_2O or D_2O , and the concentration of the nucleotide was determined by UV spectroscopy ($\lambda_{max} = 252$ nm; $\epsilon = 1.37 \times 10^4$ M $^{-1}$ cm $^{-1}$; pH 7). The required amount of gold(III) compound was added to the 5'-GMP solution.

Methods. (i) Thermogravimetric Analysis. Measurements were made on a Shimadzu TGA-50 analyzer under a N_2 atmosphere with a flow rate of 20 mL/min in a platinum cell. Samples weighed 3–7 mg. The temperature was increased at 20 °C/min from room temperature to 900 °C.

(ii) NMR. Spectra were obtained in D_2O on a Varian Inova 500-MHz spectrometer in D_2O . The temperature-dependent 1H NMR studies were referenced to an internal tetramethylammonium ion at 3.185 ppm, and the spectra at 26 °C were referenced to the HOD line at 4.800 ppm (the TMA^+ resonance is very near that of en and can overlap at times). ^{31}P NMR spectra were referenced to external 85% H_3PO_4 and ^{13}C NMR spectra to DSS. pD = pH (meter reading) + 0.40.

(iii) Electrochemical Measurements. A CHI 832 workstation (CH Instruments, Inc.) was used to collect electrochemical data. Experiments were performed at room temperature (20 ± 1 °C) in a conventional three-electrode system with a 3.0-mm-diameter glassy carbon (GC) disk working electrode (Bioanalytical Systems, Inc.), a platinum wire as the auxiliary electrode, and a $Ag/AgCl/3M$ NaCl (BAS) reference electrode. Prior to use, the GC electrodes were wet-polished on an Alpha A polishing cloth (Mark V Lab) with successively smaller particles (0.3- and 0.05- μ m diameter) of alumina. The slurry that accumulated on the electrode surface was removed by ultrasonication for 30 s in methanol and deionized water.

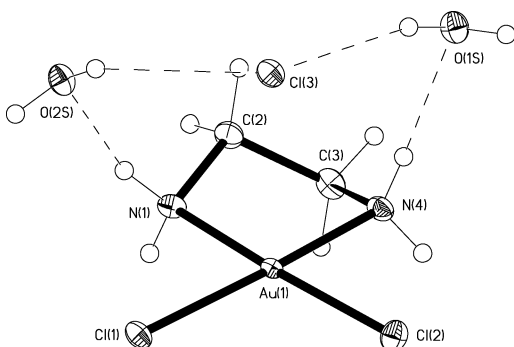
The concentration of the gold complexes was 1.0 mM, and the background electrolyte was 0.40 M NaCl. The experiments were

- (13) Gibson, D. W.; Beer, M.; Barnett, R. J. *Biochemistry* **1971**, *10*, 3669–3679.
 (14) Chatterji, D.; Nandi, U. S.; Podder, S. K. *Biopolymers* **1977**, *16*, 1863–1878.
 (15) Yang, T.; Zhang, J.-Y.; Tu, C.; Lin, J.; Liu, Q.; Guo, Z.-J. *Wuji Huaxue Xuebao* **2003**, *19*, 45–48.
 (16) Mizuno, Y.; Komiya, S. *Inorg. Chim. Acta* **1986**, *125*, L13–L15.
 (17) Marcon, G.; O'Connell, T.; Orioli, P.; Messori, L. *Met.-Based Drugs* **2000**, *7*, 253–256.
 (18) Zhu, S.; Matilla, A.; Tercero, J. M.; Vijayaragavan, V.; Walmsley, J. A. *Inorg. Chim. Acta* **2004**, *357*, 411–420.
 (19) Wirth, W.; Blotevogel-Baltronat, J.; Kleinkes, U.; Sheldrick, W. S. *Inorg. Chim. Acta* **2002**, *339*, 14–26.

Table 1. Crystallographic Data for [Au(en)Cl₂]Cl·2H₂O

chemical formula	C ₂ H ₁₂ AuCl ₃ N ₂ O ₂
fw	399.45
space group (No. 61)	<i>Pbca</i>
<i>a</i>	11.5610(15) Å
<i>b</i>	12.6399(17) Å
<i>c</i>	13.2156(17) Å
$\alpha = \beta = \gamma$	90 deg
<i>V</i>	1931.2(4) Å ³
<i>Z</i>	8
<i>T</i>	−173(2) °C
λ	0.710 73 Å
<i>D</i> _{calcd}	2.748 g/cm ³
μ	160.19 cm ^{−1}
<i>R</i> (<i>F</i> ,obsd) ^a	0.0221
<i>wR</i> (<i>F</i> ² ,all) ^a	0.0620

$$^a R = \frac{\sum ||F_o| - |F_c||}{\sum |F_o|}, wR = \left\{ \frac{\sum [w(F_o^2 - F_c^2)^2]}{\sum [w(F_o^2)^2]} \right\}^{1/2}.$$

**Figure 2.** ORTEP drawing of [Au(en)Cl₂]Cl·2H₂O with the atomic numbering scheme.

repeated at least three times, and the means of measurements are presented with the standard deviations or relative standard deviations.

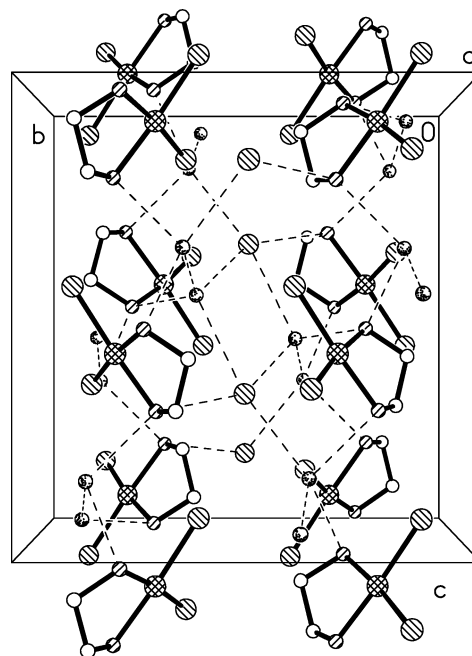
Bulk electrolysis of stirred solutions of gold complexes was performed using a GC rod (~0.6 cm²) as a working electrode. The reductive electrolysis was continued for ~4 h until the current dropped to ~1% of its initial value. The progress of electrolysis was also followed by using UV–visible spectrometry.

(iv) X-ray Structure Determination. A colorless prism-shaped crystal of dimensions 0.54 × 0.36 × 0.20 mm was selected for structural analysis. Intensity data were collected using a Bruker D8 instrument with an APEX detector and graphite-monochromated Mo K α radiation.²⁰ A total of 11 038 reflections were measured in the range of $2.84 \leq \theta \leq 26.00^\circ$ using ω -scan frames. The intensity data were corrected by a face-indexed, analytical absorption correction²¹ and an empirical absorption correction,²² giving transmittances in the range of 0.0421–0.1419. These data were merged to form a set of 1897 independent data with $R_{int} = 0.0337$ and a completion of 99.8%. The space group *Pbca* was determined by systematic absences and confirmed by refinement. The structure was solved by direct methods and refined by full-matrix least squares on F^2 .²¹ The final difference map had maxima and minima of +1.766 and −1.140 e/Å³, respectively.

(20) *SMART Software Reference Manual* and *SAINTE Software Reference Manual*; Bruker-AXS: Madison, WI, 1998.

(21) (a) Sheldrick, G. M. *SHELXTL Reference Manual*, version 6.10; Bruker-AXS: Madison, WI, 2000. (b) *International Tables for Crystallography*; Kluwer: Boston, 1965; Vol. C, Tables 6.1.1.4, 4.2.6.8, and 4.2.4.2.

(22) Sheldrick, G. M. *SADABS*; University of Göttingen: Göttingen, Germany, 2002.

**Figure 3.** Packing diagram of [Au(en)Cl₂]Cl·2H₂O.**Table 2.** Selected Bond Lengths (Å) and Angles (deg) for [Au(en)Cl₂]Cl·2H₂O

Au(1)–N(1)	2.029(4)	Au(1)–N(4)	2.030(3)
Au(1)–Cl(1)	2.2811(9)	Au(1)–Cl(2)	2.2836(11)
Au(1)–Cl(3)	3.3033(10)		
N(1)–Au(1)–Cl(1)	89.90(11)	N(4)–Au(1)–Cl(1)	173.89(10)
N(1)–Au(1)–Cl(2)	175.65(11)	N(4)–Au(1)–Cl(2)	91.27(10)
Cl(1)–Au(1)–Cl(2)	94.32(4)	N(1)–Au(1)–N(4)	84.47(15)
Cl(1)–Au(1)–Cl(3)	87.63(3)	Cl(2)–Au(1)–Cl(3)	85.30(3)

Table 3. Torsion Angles (deg) for [Au(en)Cl₂]Cl·2H₂O

N(4)–Au(1)–N(1)–C(2)	−12.3(3)
Cl(1)–Au(1)–N(1)–C(2)	170.1(2)
Cl(2)–Au(1)–N(1)–C(2)	−24.0(16)
Au(1)–N(1)–C(2)–C(3)	38.8(4)
N(1)–C(2)–C(3)–N(4)	−53.7(4)
C(2)–C(3)–N(4)–Au(1)	42.5(4)
N(1)–Au(1)–N(4)–C(3)	−16.7(3)
Cl(1)–Au(1)–N(4)–C(3)	6.4(13)
Cl(2)–Au(1)–N(4)–C(3)	162.4(3)

Results and Discussion

Structure of [Au(en)Cl₂]Cl·2H₂O. The crystal data and structure refinement are given in Table 1, and the ORTEP view and crystal packing of [Au(en)Cl₂]Cl·2H₂O are shown in Figures 2 and 3. Selected bond distances (Å) and angles (deg) are listed in Tables 2 and 3, and hydrogen bond distances are given in Table 4. The Au^{III} ion is four-coordinated in a square-planar geometry as expected. The Au–N bond lengths are 2.029(4) and 2.030(3) Å, which are roughly the same as those found in [Au(phen)Cl₂]Cl (2.03–2.06 Å)⁶ and macrocyclic polyamine complexes²³ but slightly longer than those in gold(III) peptide complexes (1.98–2.02 Å)^{24,25} and a pyridine-2-carboxamido complex.²⁶ They are slightly shorter than those in an ethylenediaminetetraacetic

(23) Suh, M. P.; Kim, I. S.; Shim, B. Y.; Hong, D.; Yoon, T.-S. *Inorg. Chem.* **1996**, *35*, 3595–3598.

(24) Wienken, M.; Lippert, B.; Zangrando, E.; Randaccio, L. *Inorg. Chem.* **1992**, *31*, 1983–1985.

Table 4. Hydrogen Bonds for [Au(en)Cl₂]Cl·2H₂O (Å and deg)

D—H···A ^a	d(D—H)	d(H···A)	d(D···A)	∠(DHA)
N(1)—H(1A)···O(2S)	0.93(6)	1.88(6)	2.791(5)	164(4)
N(1)—H(1B)···Cl(3)#1	0.80(5)	2.39(5)	3.180(4)	170(5)
N(4)—H(4A)···O(2S)#2	0.81(5)	2.04(5)	2.807(5)	157(5)
N(4)—H(4B)···O(1S)	0.82(5)	2.11(5)	2.925(5)	173(5)
O(1S)—H(1S1)···Cl(3)	0.81(5)	2.35(5)	3.135(3)	164(5)
O(1S)—H(1S2)···Cl(3)#3	0.81(6)	2.45(6)	3.243(3)	166(5)
O(2S)—H(2S1)···Cl(3)	0.66(5)	2.60(5)	3.218(3)	157(6)
O(2S)—H(2S2)···O(1S)#4	0.79(5)	2.04(5)	2.813(4)	168(5)

^a D is a hydrogen-bond donor; A is a hydrogen-bond acceptor. Symmetry transformations used to generate equivalent atoms: #1, $-x + 1/2, y + 1/2, z$; #2, $x, -y + 1/2, z + 1/2$; #3, $-x, -y, -z + 1$; #4, $x + 1/2, y, -z + 1/2$.

acid complex (2.06–2.11 Å).²⁷ The Au^{III}–Cl bond lengths for the coordinated Cl[−] are 2.2811(9) and 2.2836(11) Å, which are roughly the same as those found in the literature.^{6,11,27} The root-mean-square deviation from planarity for the five atoms comprising the square plane [N(1), N(4), Au, Cl(1), and Cl(2)] is 0.0177.

The Au^{III}–Cl(3) (ionic) distance is 3.3033(10) Å, with the Cl[−]–Au vector $\sim 90^\circ$ relative to the Au(N₂Cl₂) square plane. Although much longer than the Au–Cl covalent bond distance and a little longer than the 3.103(4) Å found by Minacheva et al.¹¹ for the square-bipyramidal [Au(en)₂Cl₂]–Cl compound, it is short enough to suggest a possible weak interaction between Cl[−] and Au^{III}. The bonding of a fifth ligand, and sometimes a sixth, to a primarily square-planar complex is well-known.²⁸ An unusual compound, Au(2,2'-bpy)Cl₃·2.25H₂O, where 2,2'-bpy is 2,2'-bipyridine, has been reported by Lippert et al., in which two square-planar [Au(bpy)Cl₂]⁺ ions are connected by a long Au–Cl–Au bridge [average Au–Cl of 3.218(3) Å].²⁹ Because the bpy ligands in the two units are said to be parallel to each other, it is likely that π stacking holds the units sufficiently close to allow bridging.

The N(1)–Au–N(4) bond angle is 84.47(15)°, while the Cl(1)–Au–Cl(2) bond angle is 94.32(4)°. The difference between these is expected because of the greater nonbonding-to-nonbonding electron-pair repulsions between the two coordinated Cl atoms. The same type of variation as that between the N_a–Au–N_b and Cl_a–Au–Cl_b bond angles was reported for [Au(phen)Cl₂]Cl,⁶ although both bond angles were smaller than those we report for [Au(en)Cl₂]Cl·2H₂O. The Au–N and Au–Cl bond lengths and the Cl–Au–Cl and N–Au–N angles are comparable with those of the Au₂(trien)Cl₅ complex, where trien is triethylenetetraamine.³⁰

The cations and water molecules crystallize in layers in the *b* direction. A layer of chlorides separates every two

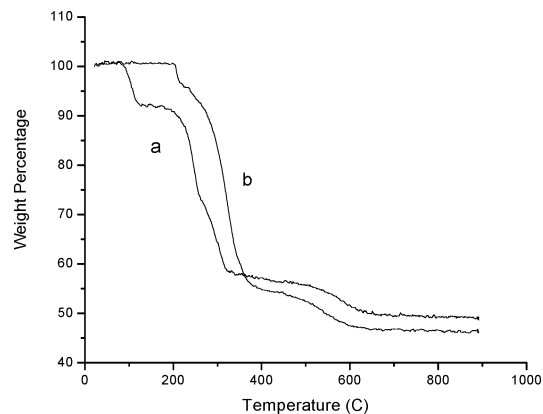
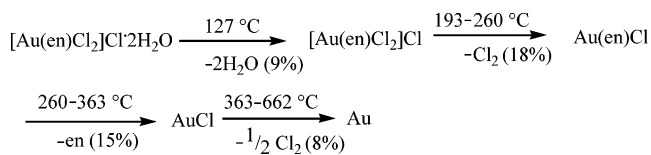


Figure 4. Thermogravimetric analysis curves of (a) [Au(en)Cl₂]Cl·2H₂O and (b) [Au(en)₂Cl₂]Cl·0.5HCl run in a N₂ atmosphere with a flow rate of 20 mL/min and a temperature increase of 20 °C/min.

Scheme 1



layers of the cations and waters. There is extensive hydrogen bonding between the NH₂, Cl(3), and water of hydration, which serves to stabilize the structure (Table 4). As shown in Figure 3, two water molecules are associated with each other through a hydrogen bond. One of the pairs (H₂O(1S)) also forms hydrogen bonds to two Cl(3) and to the N of one en. The other H₂O(2S) hydrogen bonds to one Cl(3) and to en in two different cations. There is additional hydrogen bonding between NH₂ and Cl(3).

Thermal Analysis. As shown in Figure 4, [Au(en)Cl₂]–Cl·2H₂O loses its water of hydration beginning at 77 °C, and all water is lost by 127 °C. The 9% weight loss agrees with the loss of 2 mol of water. Scheme 1 gives the temperature ranges of the decompositions, the experimental mass losses, and the products.

[Au(en)₂]Cl₃·0.5HCl behaves in a similar manner. After loss of 0.5 mol of HCl (4%), it loses two Cl and two en (42%) between 220 and 390 °C, and the remaining AuCl decomposes between 390 and 600 °C. The en and Cl are lost at a higher temperature in Au(en)₂Cl₃·0.5HCl than in [Au(en)Cl₂]Cl·2H₂O, probably because of the stronger coordination of the en ligand compared to the Cl[−] ligand.

Electrochemistry of Gold Complexes. The survey cyclic voltammograms recorded at GC electrodes in aqueous solutions of gold complexes (1.0 mM in 0.40 M NaCl) displayed a series of distinct current peaks: A, B, B1, and C (Figure 5). The original reduction peak A shifted toward more negative potentials in the order $E_p(\text{AuCl}_4^-)$, 0.410 V $> E_p[\text{Au(en)Cl}_2^+]$, 0.140 V $> E_p[\text{Au(en)}_2^{3+}]$, −0.290 V. This indicated that a bidentate en ligand stabilized the Au^{III} oxidation state against reduction, as was previously reported for chelating N donor ligands.³¹ The positions of peaks B,

(25) Best, S. L.; Chattopadhyay, T. K.; Djuran, M. I.; Palmer, R. A.; Sadler, P. J.; Sovago, I.; Varnagy, K. *J. Chem. Soc., Dalton Trans.* **1997**, 2587–2596.

(26) Hill, D. T.; Burns, K.; Titus, D. D.; Girard, G. R.; Reiff, W. M.; Mascavage, L. M. *Inorg. Chim. Acta* **2003**, *346*, 1–6.

(27) Cornejo, A. A.; Castineiras, A.; Yanovsky, A. I.; Nolan, K. B. *Inorg. Chim. Acta* **2003**, *349*, 91–96.

(28) Marangoni, G.; Pitteri, B.; Bertolasi, V.; Ferretti, V.; Gilli, G. *J. Chem. Soc., Dalton Trans.* **1987**, 2235–2240.

(29) Micklitz, W.; Lippert, B.; Müller, G.; Mikulcic, P.; Riede, J. *Inorg. Chim. Acta* **1989**, *165*, 57–64.

(30) Messori, L.; Abbate, F.; Orioli, P.; Tempi, C.; Marcon, G. *Chem. Commun.* **2002**, 612–613.

(31) Messori, L.; Abbate, F.; Marcon, G.; Orioli, P.; Fontani, M.; Mini, E.; Mazzei, T.; Carotti, S.; O'Connell, T.; Zanello, P. *J. Med. Chem.* **2000**, *43*, 3541–3548.

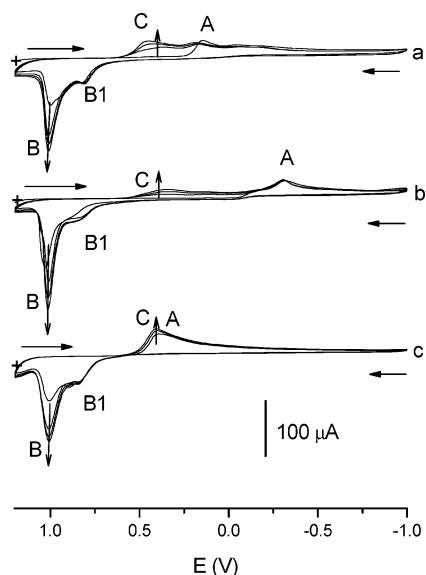


Figure 5. Survey cyclic voltammograms recorded at a GC electrode in 1.0 mM solutions of gold(III) complexes: (a) Au(en)Cl_2^+ ; (b) Au(en)_2^{3+} ; (c) AuCl_4^- . The vertical arrows indicate a direction of change in the peak currents upon repetitive scanning of the electrode potential. Background electrolyte: 0.40 M NaCl. Scan rate: 100 mV/s.

B1, and C, which developed on consecutive voltammetric scans, were essentially not influenced by the composition of the gold complex. The gold complexes displayed good electrochemical stability as indicated by their peak currents and peak potentials, which were stable ($\pm 10\%$) at least for 4 h.

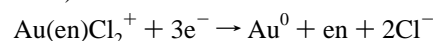
The origin of the current peaks can be conveniently discussed by using the cyclic voltammogram for the Au(en)Cl_2^+ complex (Figure 5a) as an example. On the first cathodic (negative-going) potential scan, the current peak A at 0.14 V was formed because of the reduction of the gold complex. The reduction process involved three electrons per molecule ($n = 3$), as indicated by the coulometric analysis of the exhaustive electrolysis at 0.0 V. The $\text{Au}^{\text{III}} \rightarrow \text{Au}^0$ reduction was also confirmed by the presence of a gold deposit on the electrode surface after the electrolysis. The voltammetric and chronoamperometric analyses showed no intermediate gold(I) complexes, which is compatible with the fact that the en is not a π -acceptor ligand that could stabilize the intermediate oxidation state of gold. Such stabilization has been demonstrated in the case of gold complexed with the π -acceptor phosphine ligands.³²

On the anodic (positive-going) backward scan, a symmetrical current peak B was formed at ~ 1.00 V. This peak was present only when the potential on the forward scan was scanned beyond peak A. Thus, peak B was ascribed to anodic dissolution $\text{Au}^0 \rightarrow \text{Au}^{\text{III}}$ of the gold deposit. In the presence of high chloride concentration in the solution, the anodic stripping of the Au^0 deposit was driven by the complexation of Au^{III} ions with Cl^- ions. A small peak B1 that appeared at ~ 0.80 V was probably due to the competing process of gold oxide formation. The current after peak B did not decay to zero, which suggested that the formation

of gold oxide precluded a total dissolution of the Au^0 deposit from the electrode surface.

The scanning of the potential again toward more negative values yielded a broad reduction peak C at ~ 0.40 V, which was not present during the first cathodic scan. Peak C can be ascribed to two parallel processes, which involved the reduction of gold oxide and the AuCl_4^- complex that were formed at the electrode/solution interface during the preceding anodic scan. The supportive argument for the latter process was that the reduction of the AuCl_4^- reference complex yielded a current peak (Figure 5c, peak A) at the same potential as that of peak C. The foregoing discussion can be summarized by the following overall peak assignments:

Peak A (0.14 V, cathodic):

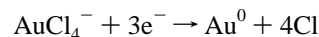
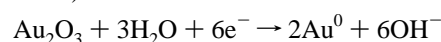


Peak B (1.0 V, anodic): $\text{Au}^0 + 4\text{Cl}^- \rightarrow \text{AuCl}_4^- + 3e^-$

Peak B1 (0.80 V, anodic):



Peak C (0.40 V, cathodic):



Such an interpretation of peaks B, B1, and C is in agreement with the independence of the peak potentials upon the composition of the starting gold complex.

To avoid complications from excessive deposition/dissolution processes, the AuCl_4^- , $[\text{Au(en)Cl}_2]^+$, and $[\text{Au(en)}_2]^{3+}$ complexes were studied in narrower potential windows that included only their original reduction peak A (Figure S1 in the Supporting Information). The analysis of the scan rate (v) dependence of the peak currents (I_p) and peak potentials (E_p) revealed that I_p increased linearly with $v^{1/2}$ ($R^2 = 0.997 - 0.994$) and E_p was directly proportional to $\log(v)$ ($R^2 = 0.998 - 0.991$) while shifting toward higher overpotentials. This indicated that molecules of gold complexes were transported by diffusion to the electrode surface, where they underwent electrochemically irreversible reduction. The voltammetry and chronoamperometry revealed that the substitution of Cl^- ions with bulkier en ligands resulted in a lowering of the diffusion coefficient (Table 1S in the Supporting Information).

Interaction with 5'-GMP. The AuCl_4^- ion and other gold(III) chloro complexes are known to undergo hydrolysis in water at relatively low pH.^{7,13} $[\text{Au(en)Cl}_2]\text{Cl}$ hydrolyzed in an aqueous solution above pD ~ 2.5 , as shown by changes in the ^1H NMR of the en ligand (Figure S2 in the Supporting Information). At pD 1.4, the en chemical shift was 3.28 ppm, which is assigned to the $[\text{Au(en)Cl}_2]^+$ complex. At pD 3.4, a new line appeared at 3.30 ppm and the intensity of the 3.28 ppm resonance was greatly reduced. The NMR line at 3.0 ppm is likely to be a hydroxo complex, such as Au(en)(OH)Cl^+ or Au(en)(OH)_2^{+6} . At the even higher pD of 5.8, three distinct species were present (3.22, 3.27, and 3.30 ppm)

(32) Koelle, U.; Laguna, A. *Inorg. Chim. Acta* **1999**, *290*, 44–50.

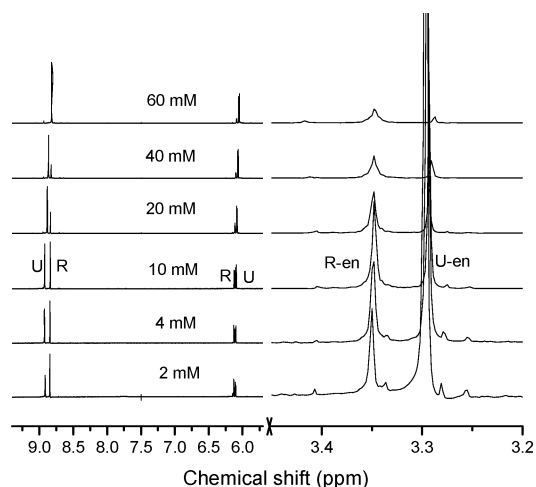


Figure 6. ^1H NMR of 10 mM $[\text{Au}(\text{en})\text{Cl}_2]\text{Cl}$ with various concentrations of $\text{H}_2(5'\text{-GMP})$ in D_2O , pD 2.5. U = unreacted $5'\text{-GMP}$; R = $\text{Au}(\text{en})\text{-GMP}$ complex.

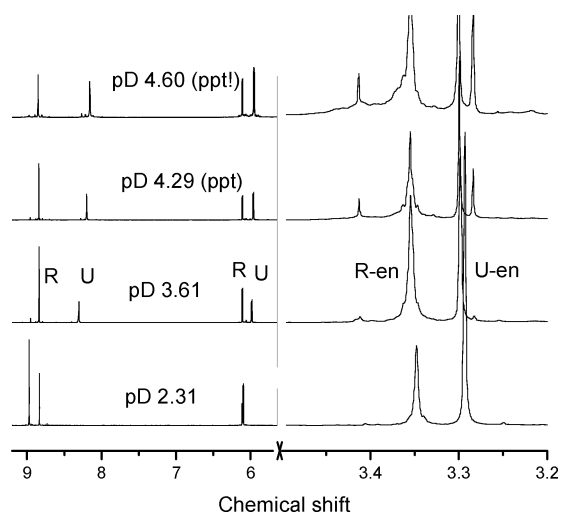


Figure 7. ^1H NMR of 10 mM $\text{Au}(\text{en})\text{-}5'\text{-GMP}$ in D_2O at various pD. U = unreacted $5'\text{-GMP}$; R = $\text{Au}(\text{en})\text{-GMP}$ complex.

and a brown precipitate was observed, which precluded continuing above pD 5. This precipitate contained no en or $5'\text{-GMP}$ and was assumed to be an oxide or hydroxide of gold(III). A line at 3.22 ppm was broad and was probably a soluble polymeric gold(III) hydroxo or oxo species.

The ^1H NMR spectra of 10 mM aqueous solutions of $[\text{Au}(\text{en})\text{Cl}_2]\text{Cl}$ containing different amounts of $5'\text{-GMP}$ in an acidic solution are shown in Figure 6. There are clearly two $5'\text{-GMP}$ H8 signals and two H1' signals, one each from unreacted $\text{H}_2(5'\text{-GMP})$ and from an $\text{Au}(\text{en})\text{-}5'\text{-GMP}$ complex. The upfield of the two H8 (8.84 ppm) resonances and the downfield of the two H1' (6.13 ppm) resonances are assigned to $\text{Au}(\text{en})\text{-}5'\text{-GMP}$, while the other H8 (8.92 ppm) and H1' (6.09 ppm) signals are those of unreacted $5'\text{-GMP}$. The unreacted $5'\text{-GMP}$ resonance assignments were made on the basis of a pD-dependent experiment (Figure 7), which clearly showed the expected upfield shift of the H8 line of unreacted $5'\text{-GMP}$ with increasing pD.¹⁸ Even in the 2 mM $5'\text{-GMP}$ solution where there was a 5-fold excess of $[\text{Au}(\text{en})\text{Cl}_2]\text{Cl}$, a considerable amount of unreacted $\text{H}_2(5'\text{-GMP})$ was still present. This indicates that either the stability constant of the $\text{Au}(\text{en})\text{-}5'\text{-GMP}$ complex is rather small or the acidity

Table 5. ^{13}C NMR Chemical Shifts of $5'\text{-GMP}$ and $\text{Au}(\text{en})\text{-}5'\text{-GMP}$ in D_2O at pD 2.8

	$5'\text{-GMP/ppm}^a$	$\text{Au}(\text{en})\text{-}5'\text{-GMP complex/ppm}^{b,c}$
C(6)	156.49	156.60, 156.38
C(2)	155.20	155.27, 155.25
C(4)	150.36	150.34
C(8)	136.31	139.21, 136.26
C(5)	110.95	112.65, 110.69
C(1')	89.01 ^d	90.31, 89.14
C(4')	84.19 ^e	84.40 ^e , 84.19 ^e
C(2')	74.60	74.92, 74.63
C(3')	69.82	69.78, 74.63
C(5')	63.84 ^f	64.00, 63.66
en (react)		51.87, 50.90
en (unreact)		51.13

^a 15 mM. ^b 11 mM. ^c The more downfield line is $5'\text{-GMP}$ in $\text{Au}(\text{en})\text{-}5'\text{-GMP}$, and the upfield line is unreacted $5'\text{-GMP}$. ^d Doublet, $J = 1.0$ Hz. ^e Split by ^{31}P , $J = 8.7$ Hz. ^f Split by ^{31}P , $J = 5.0$ Hz.

of the solution is such that the N(7) of $5'\text{-GMP}$ is partially protonated, or possibly both. Integration of the NMR spectra in Figure 6 shows that the mole ratio of reacted $5'\text{-GMP}$ to reacted $[\text{Au}(\text{en})\text{Cl}_2]\text{Cl}$ remained at 1:1, irrespective of the amounts of the two components in the solution. Although it appears (Figure 6) that the concentration of the $\text{Au}(\text{en})\text{-}5'\text{-GMP}$ complex is decreasing with increasing $5'\text{-GMP}$ concentration, it is simply the large excess of $5'\text{-GMP}$ that gives that appearance in the spectra.

The pD study of a solution of 20 mM $\text{Au}(\text{en})\text{Cl}_3$ containing 20 mM $5'\text{-GMP}$ was carried out over the pD range of 2.3–4.6 (Figure 7). Some precipitate of the hydrolyzed gold(III) species was observed at pD 4.3 and above. The chemical shift of the H8 signal of the $\text{Au}(\text{en})\text{-GMP}$ complex remained constant at 8.83 ppm over the pD range studied, but that of unreacted $5'\text{-GMP}$ gradually shifted upfield with increasing pD until it reached 8.2 ppm, the chemical shift at which N(7) is completely deprotonated. It is well-known that metal–N(7) purine bonding causes a large downfield shift of the H8 resonance. Therefore, the fact that the H8 resonance in the $\text{Au}(\text{en})\text{-GMP}$ complex remained constant at 8.83 ppm proves that Au^{III} is bonding to the N(7) of $5'\text{-GMP}$. The ^{31}P NMR of solutions under the same conditions and pD 3.6 also showed two resonances, 0.88 ppm (unreacted $5'\text{-GMP}$) and 0.53 ppm (reacted $5'\text{-GMP}$). Although this indicated a slightly different environment for the bonded $5'\text{-GMP}$, it showed that a possible N(7)–phosphate macrochelate structure was not being formed because the ^{31}P NMR resonance for $\text{Au}^{\text{III}}\text{-OPO}_3\text{R}$ bonding would be located considerably downfield, as was observed in a $\text{Co}^{\text{III}}\text{-}5'\text{-GMP}$ complex at 12 ppm.³³

The NMR results strongly support the formation of a 1:1 complex of a monomeric $\text{Au}^{\text{III}}(\text{en})$ complex with monodentate N(7)–GMP bonding and a fourth ligand of Cl^- , OH^- , or water. Alternatively, a N(7)–O(6) chelate structure, proposed but not confirmed by several authors,^{13,14} could be formed. To determine the presence of this type of bonding, the ^{13}C NMR spectrum of 11 mM $\text{Au}(\text{en})\text{Cl}_3\text{-GMP}$ (1:1 mole ratio) in D_2O at pD 2.8 was run and compared with that of $5'\text{-GMP}$ under the same conditions (Table 5 and Figure S3

(33) Fletcher, T. M.; Walmsley, J. A. *J. Inorg. Biochem.* **1997**, *68*, 239–249.

in the Supporting Information). As was observed for the ^1H NMR spectrum of $\text{Au}(\text{en})\text{Cl}_3\text{-GMP}$ (1:1 mole ratio), lines were present for both complexed and unreacted $\text{H}_2(5'\text{-GMP})$. In all cases, the resonances of the complexed species were located downfield of the corresponding resonances of the unreacted $5'\text{-GMP}$. The only ^{13}C NMR resonances that exhibited significant differences in the chemical shifts between the complexed and unreacted species were C(8) ($\Delta\delta = 2.9$ ppm), C(5) ($\Delta\delta = 1.6$ ppm), and C(1') ($\Delta\delta = 1.3$ ppm). The relatively large $\Delta\delta$ values for the C(8) and C(5) carbons flanking the N(7) position is just what is expected for $\text{Au}^{\text{III}}\text{-N}(7)$ GMP bonding, while the small $\Delta\delta$ of 0.1 ppm for C(6) suggests that $\text{C}=\text{O}$ is not involved in the bonding. Therefore, these data eliminate the $\text{N}(7)\text{-O}(6)$ chelate structure as a possible Au^{III} bonding mode at pD 2.8. The $\Delta\delta$ for C(1') was ascribed to a conformational change of the ribose in the complexed species. These data also confirm that bonding of the $\text{Au}(\text{en})$ moiety is to the N(7) of $5'\text{-GMP}$.

The thermal stability of a solution, which was 10 mM in $[\text{Au}(\text{en})\text{Cl}_2]\text{Cl}$ and 15 mM in $\text{H}_2(5'\text{-GMP})$ (pD 2.4), was investigated over the temperature range of 2–50 °C. The complex decomposed slightly as the temperature was raised, decreasing from 33% $[\text{Au}(\text{en})\text{Cl}_2]\text{Cl}$ reacted at 2 °C to 27% reacted at 50 °C. This implies that the coordination of $5'\text{-GMP}$ to $[\text{Au}(\text{en})\text{Cl}_2]^+$ is an exothermic process.

As one might expect, there is no significant reaction between $\text{Au}(\text{en})_2\text{Cl}_3$ and $\text{Na}_2(5'\text{-GMP})$. The only ^1H NMR signals of $5'\text{-GMP}$ observed were those typical of an unreacted nucleotide. This is due to the fact that the two coordinated bidentate en ligands bind to Au^{III} more strongly than $5'\text{-GMP}$. Although no direct coordination of $5'\text{-GMP}$ was observed in the $\text{Au}(\text{en})_2\text{Cl}_3\text{-GMP}$ system, hydrogen bonding between $5'\text{-GMP}$ and the en in the $\text{Au}(\text{en})_2\text{Cl}_3$ complex, as reported for other coordinatively saturated complexes,^{33,34} cannot be ruled out.

Acknowledgment. The authors thank the National Institutes of Health (NIGMS/SCORE program, Grant SO6-08194) and The University of Texas at San Antonio for research support.

Supporting Information Available: Crystallographic data file in CIF format, cyclic voltammetry as a function of the scan rate, diffusion coefficients, ^1H NMR of $[\text{Au}(\text{en})\text{Cl}_2]\text{Cl}$ as a function of pD, and ^{13}C NMR available. This material is available free of charge via the Internet at <http://pubs.acs.org>.

IC051411P

(34) Farmer, P. J.; Cave, J. R.; Fletcher, T. M.; Rhubottom, J. A., Jr.; Walmsley, J. A. *Inorg. Chem.* **1991**, *30*, 3414–3420.